ELSEVIER

Biochimica et Biophysica Acta 1565 (2002) 287–293

BIOCHIMICA ET BIOPHYSICA ACTA
BBA

www.bba-direct.com

Review

The structure of the M2 channel-lining segment from the nicotinic acetylcholine receptor☆

M. Montal[a,*], S.J. Opella[b]

[a] *Section of Neurobiology, Division of Biology, University of California San Diego, 9500 Gilman Drive, La Jolla, CA 92093-0366, USA*
[b] *Department of Chemistry and Biochemistry, University of California San Diego, La Jolla, CA, USA*

Received 5 January 2002; received in revised form 3 May 2002; accepted 3 May 2002

Abstract

The structures of functional peptides corresponding to the predicted channel-lining M2 segment of the nicotinic acetylcholine (AChR) were determined using solution NMR experiments on micelle samples, and solid-state NMR experiments on bilayer samples. The AChR M2 peptide forms a straight transmembrane α-helix, with no kinks. M2 inserts in the lipid bilayer at an angle of 12° relative to the bilayer normal, with a rotation about the helix long axis such that the polar residues face the N-terminus of the peptide, which is assigned to be intracellular. A molecular model of the AChR channel pore, constructed from the solid-state NMR 3-D structure of the AChR M2 helix in the membrane assuming a pentameric organization, results in a funnel-like architecture for the channel with the wide opening on the N-terminal intracellular side. A central narrow pore has a diameter ranging from about 3.0 Å at its narrowest, to 8.6 Å at its widest. Nonpolar residues are predominantly on the exterior of the bundle, while polar residues line the pore. This arrangement is in fair agreement with evidence collected from permeation, mutagenesis, affinity labeling and cysteine accessibility measurements. A pentameric M2 helical bundle may, therefore, represent the structural blueprint for the inner bundle that lines the channel of the nicotinic AChR.

Keywords: Neurotransmitter receptor; Ion channel; Membrane protein; NMR; Structure

1. Perspectives and overview

Neurons communicate with each other by means of neurotransmitters [1]. The vast and intricate connectivity of the human brain combined with the diversity of neurotransmitters is at the root of the combinatorial power that contributes to the dynamic complexity of the brain. Synaptic communication is tightly regulated and, accordingly, alterations lead to dysfunction, which range from developmental abnormalities to aberrant behavior. Ostensibly, the proteins involved in the process are membrane proteins or membrane associated proteins and still little is known about their molecular structure, dynamics and interactions. Our research is focused on channel proteins, which are pivotal components of this fascinating system, and the models currently in vogue to understand how their structure produces their function or dysfunction.

The expectation that well in excess of 1000 new potential drugs in the field of neuroscience will be derived from genomics and that >90% of these will be targeted to channels and receptors will require structural knowledge of the drug binding pocket. This fertile field provides an unparalleled opportunity to blend the power of structural biology and membrane biophysics in order to define the folds adopted by channel proteins to fulfill their function and to facilitate drug design targeted to block or modulate channel activity arising from dysfunctional channels.

The thrust of our research aims to establish structure–function relationships in channel proteins with a primary emphasis on the transmembrane domain. Even today, there is only a handful of high-resolution structures of channel proteins, a major gap in our knowledge about this class of proteins that are critical for signaling in cells. These structures, excluding the bacterial porins, are for KcsA-a K^+ channel of *S. lividans* [2], *MscL*—a mechanosensitive

☆ The coordinates of the solution and solid state NMR structures of the AChR M2 are available in the Protein Data Bank (PDB file 1A11).

* Corresponding author. Tel.: +1-858-534-0931; fax: +1-858-822-3763.
E-mail address: mmontal@ucsd.edu (M. Montal).

0005-2736/02/$ - see front matter © 2002 Elsevier Science B.V. All rights reserved.
PII: S0005-2736(02)00575-8

channel of *Mycobacterium tuberculosis* [3], *GlpF*—a glycerol-conducting channel from *Escherichia coli* [4], the AQP1 water channel [5], and two bacterial chloride channels from the CLC family [6], all determined by X-ray crystallography. We have applied solid-state NMR methods to elucidate the structures of several channel proteins. A unique advantage of solid-state NMR methods is that protein structure is determined in the lipid bilayer, which is the biologically relevant environment for membrane proteins. NMR spectroscopy is ideally suited to probe protein dynamics, a feature of utmost importance in systems such as channel proteins where conformational transitions are at the core of their biological action.

Our initial studies have been an integral part of the development of the NMR approach to structure determination of membrane proteins, and they have been focused on functional 25-residue peptides corresponding to the pore forming elements of acetylcholine receptors (AChR), glycine receptors (GlyR), and glutamate receptors (GluR). These functional peptides have enabled us to formalize a hierarchical approach to structure. However, our ultimate goal is to build upon these results to study intact functional ion-channels. Although multidimensional solution NMR methods can be successfully applied to relatively small membrane proteins in micelles in favorable cases [7], the size limitation is more severe than for globular proteins because the lipid molecules associated with each polypeptide slow the overall reorientation rate. Moreover, it is highly desirable to determine the structures of membrane proteins in the definitive environment of phospholipid bilayers where solution NMR methods fail completely. Recently, we determined the 3-D structure of a 25-residue M2 channel forming peptide from AChRs by solid-state NMR spectroscopy [8]. We turn now to summarize the key features of this endeavor.

2. The nicotinic acetylcholine receptor channel

Our focus has been on neurotransmitter-gated ion channels, a superfamily of oligomeric proteins in the postsynaptic membrane of neurons which are responsible for neuronal communication [1,9], and specifically on the channel-forming domain confined to the membrane. The nicotinic AChR has been one of the most extensively studied members of a growing superfamily of ligand-gated channels [10,11]. It is a pentamer of homologous subunits organized around a central aqueous pore. The ligand-binding domain is exposed to the extracellular surface and is largely formed by the N-terminal region of the α subunits. Two agonist binding sites are formed at the interface between the two α subunits and the adjacent subunit-α and γ, and α and δ subunits for the muscle AChR, or between adjacents α subunits for the homopentameric α7 neuronal AChR.

The recent crystal structure of a snail ACh-binding protein (AChBP) [12] that is secreted from the molluscan glial cells and has sequence similarities to the N-terminal domain of the nicotinic AChR has revealed the essential features of this extramembranous domain, supporting a modular design. Remarkably, the structure of the AChBP homopentamer solved at 2.7 Å resolution compares favorably with the corresponding domain in the 4.6 Å structure of the *Torpedo marmorata* AChR determined by cryo-EM combined with image reconstruction [13]. It also accounts for a plethora of biochemical, mutagenesis and electrophysiological information. Each protomer in the pentamer adopts a modified immunoglobin fold with a core of 10 twisted β strands that generate two separate hydrophobic cores. The pentamer has a central hydrophilic pore of ~ 20 Å in diameter, lined with charged residues. There is a cavity at each interface between the five subunits lined by hydrophobic residues and formed by four loops (A–D), which were previously identified in biochemical experiments as constituents of the AChR ACh binding site [14]. The binding pocket for ACh in AChBP is created by five aromatic residues: a Tyr on loop A, a conspicuous Trp on loop B, two Tyr separated by seven residues on loop C, and a Trp on loop D. It is not clear how the ligand binding event in this surface exposed module is transmitted to the channel forming domain embedded within the membrane bilayer to trigger channel opening. However, the structure of the AChBP suggests that such a ligand-binding module is well suited to interact specifically with the pore module and it provides a structural framework to pursue an understanding of the elusive coupling between ligand binding and channel opening.

What, then, do we know about the AChR transmembrane domain? A canonical structure suggests the occurrence in each subunit of four potential TMs, M1–M4. The membrane domain has high sequence similarity among members of this gene superfamily which encompasses receptors for the major inhibitory neurotransmitters glycine and GABA (γ-amino butyric acid). In particular, the high conservation of the M2 sequence and its amphipathic character suggested its dominant contribution to the structure that actually lines the channel. This assignment is compatible with a large body of evidence derived primarily from mutagenesis and affinity-labeling experiments [10,11,15–20]. The 9 Å structure of the *T. marmorata* AChR determined by Unwin [21,22] using cryo-EM combined with image reconstruction indicated the presence of only one rod of density compatible with a single transmembrane helix in each receptor subunit. The inner bundle that lines the pore was postulated to be formed by M2 helices whereas the outer rim of three-stranded antiparallel β-sheets may be contributed by M1, M3, and/or M4. The 4.6 Å structure [13] has not unequivocally identified the secondary structure of M1, M3, and M4. Evidence derived from CD [23] and infrared spectra of transmembrane domain preparations is consistent with the occurrence of four transmembrane helices in each subunit [24]. This issue will likely be resolved when the much anticipated higher resolution structure derived from Unwin's

[21] recent technical refinements and additional averaging becomes available in the near future.

3. M2 structural studies

Focusing on M2, both the 9 and 4.6 Å electron diffraction maps suggest a model in which the channel pore is formed by a bundle of five M2 α-helices, each contributed by one subunit of the AChR pentamer [13,21,22]. This model is compatible with conformational energy calculations refined using molecular dynamics [25–27], mutagenesis and substituted cysteine accessibility data [10,11,15–20]. The total chemical synthesis of a five-helix bundle protein designed to imitate this motif has been achieved [28,29]. The designed protein approximates some of the permeation properties of the authentic *T. californica* AChR reconstituted in lipid bilayers, including single channel conductance, cation selectivity and channel blockade. From a minimalist viewpoint, it seems that this fold would support the fundamental function of the AChR channel. Is it possible to determine the 3-D structure of the M2 channel-lining segment in a membrane?

This has been achieved: It is the first high-resolution structure of a functional module derived from a eukaryotic channel protein in a membrane. The 3-D structure of a functional peptide corresponding to the M2 segment from the δ-subunit of the AChR was determined by solution and solid-state NMR spectroscopy in membrane environments [8,30]. These studies exemplify an essential feature of our approach, which is the direct correlation of the structures obtained by NMR spectroscopy in micelles and bilayers with the functional properties of the channels recorded after reconstitution of the same polypeptides into bilayers. Isotopically labeled M2 peptides required for NMR spectroscopy were prepared by expression of recombinant peptides in *E. coli*, for selective or uniform isotopic labeling, or by solid-phase synthesis, for specific residue labeling of the samples.

The AChR M2 peptide forms cation-selective channels in lipid bilayers (Fig. 1a). The channels display heterogeneous conductances and lifetimes, as expected for monomeric peptides that self-assemble into conductive oligomers of discrete yet variable size. The channels that occur most frequently exhibit a single-channel conductance (γ) of 37 ± 2 pS in 0.5 M NaCl. The currents of closed (C) and open (O) states are indicated by the solid lines. Dotted lines define the range set to discriminate the transitions between states, based on signal-to-noise measurements. Conductances were calculated from the corresponding Gaussian fits to current histograms; the respective probabilities (P) of the open (O) versus closed (C) channel states are indicated (Fig. 1b). The results indicate that both the recombinant and synthetic AChR M2 peptides used in the NMR experiments are functional, and form sequence-specific, discrete ion-channels

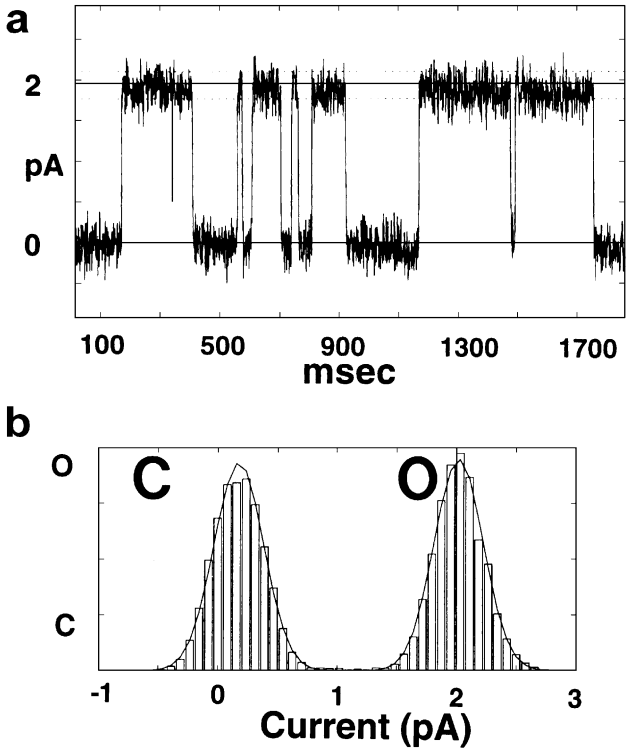

Fig. 1. (a) Single channel recordings from recombinant AChR M2 peptides in lipid bilayers. The currents were recorded at 50 mV in symmetric 0.5 M NaCl supplemented with 1 mM $CaCl_2$, 5 mM Hepes pH 7.4. The currents of closed (C) and open (O) states are indicated by the solid lines. The single channel conductance was 37 ± 2 pS. (b) Corresponding current histogram. The Gaussian fit of the data indicates the respective probabilities of the open (O) versus closed (C) channel states.

in lipid bilayers [8]. To the extent that the peptides mimic the predicted channel lining sequence (EKMSTAISVLLAQAVFLLLTSQR), their permeation properties compare favorably with those of the intact homomeric AChR.

The 2-D solution $^{1}H/^{15}N$ HMQC (heteronuclear multiple quantum correlation) NMR spectrum of uniformly ^{15}N-labeled AChR M2 peptide in dodecylphosphocholine (DPC) micelles is well resolved, with each amide resonance characterized by isotropic ^{1}H and ^{15}N chemical shift frequencies (Fig. 2a). The 2-D solid-state PISEMA [8,30] (polarization inversion spin exchange at the magic angle) spectrum of the same peptide in oriented bilayers (Fig. 2b) is well resolved, with each amide resonance characterized by ^{15}N chemical shift and $^{1}H-^{15}N$ dipolar coupling frequencies. The parallel development of solution NMR spectroscopy of lipid micelle samples and solid-state NMR spectroscopy of oriented lipid bilayer samples to yield high-quality spectra with similar resolution is of paramount significance. The primary constraint used for structure determination by solution NMR spectroscopy is the homonuclear $^{1}H/^{1}H$ NOE. The 10 lowest energy structures that satisfy the NMR data, with no NOE violations greater than 0.5 Å and no dihedral angle violations greater than 5°, and maintain acceptable peptide geometry, are shown

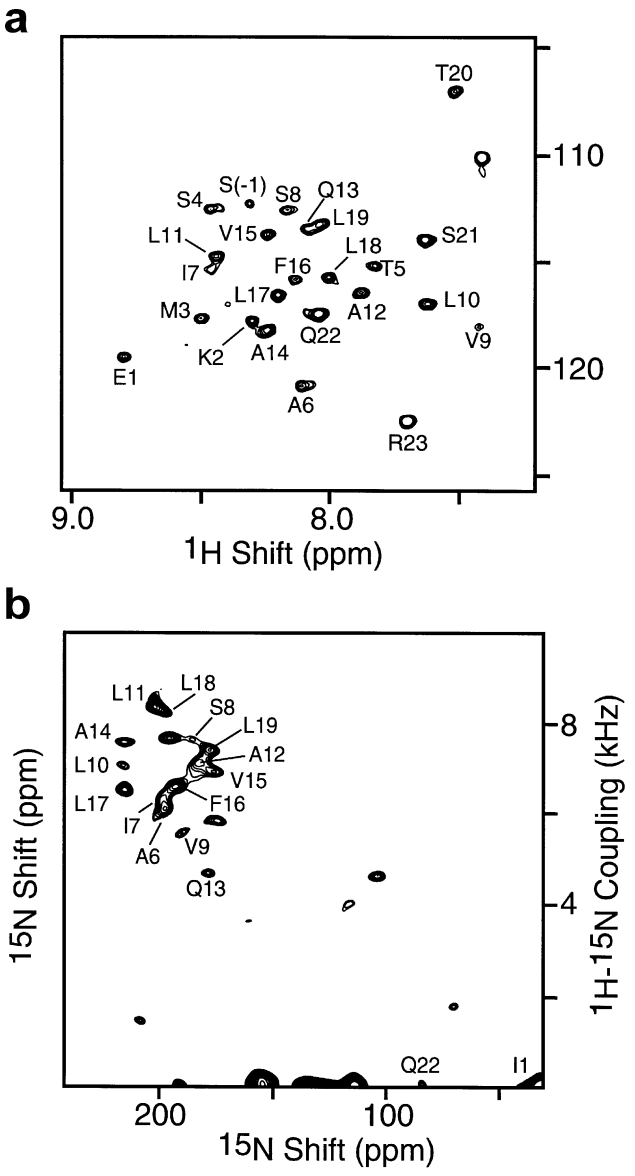

Fig. 2. (a) Solution ^{1}H chemical shift/^{15}N chemical shift correlation HMQC NMR spectrum of AChR M2 in DPC micelles, at 20 °C. Four transients were acquired for each of 256 t_1 increments. (b) Solid-state $^{1}H-^{15}N$ dipolar/^{15}N chemical shift correlation PISEMA NMR spectrum of AChR M2 in oriented DMPC bilayers, at 22 °C. Two hundred and fifty-six transients were acquired for each of 64 t_1 values incremented by 40.8 μs.

in Fig. 3a. The structures overlay best from residues Lys-2 to Gln-22 where the average RMSD of the heavy atoms of the backbone from the average structure is 0.77 ± 0.2 Å. The results show that the AChR M2 peptide adopts an α-helical structure in DPC micelles, which is only slightly curved and show no evidence of kinks.

Solid-state NMR spectroscopy on oriented lipid bilayer samples is unique in determining the complete topology, including 3-D structure and global orientation, of the peptide in the membrane, at high resolution [31,32]. The orientationally dependent ^{15}N chemical shift and $^{1}H-^{15}N$ dipolar coupling frequencies provide orientational constraints for structure determination of ^{15}N labeled peptides in lipid bilayer membranes, and can be measured directly from the 2-D PISEMA spectrum of the AChR M2 peptide (Fig. 2b). In this spectrum, the presence of a single resonance for each individual residue implies that the AChR M2 peptides adopt a single conformation in the lipid bilayer. Most of the resonances in Fig. 2b were assigned to specific residues through comparisons with spectra from selectively ^{15}N-labeled recombinant peptides, and specifically ^{15}N-labeled synthetic peptides. Some resonances were assigned with ^{15}N dilute spin-exchange experiments. The backbone structure of AChR M2, determined from ^{15}N chemical shift, $^{1}H-^{15}N$ dipolar coupling, and some ^{1}H chemical shift constraints, is shown in Fig. 3b. Superposition of the solution (black) and solid-state (cyan) NMR structures shows that they are similar, with an RMSD of 0.6 Å for the backbone atoms.

Using the solid-state NMR orientational constraints, we determined that the AChR M2 peptide is a transmembrane, amphipathic α-helix with its long helix axis tilted 12° from the lipid bilayer normal [8], in agreement with the structure inferred from the 9 and 4.6 Å electron diffraction maps [13,21,22]. The peptide is rotated around its helix long axis such that the polar residues face the N-terminus of the peptide, which is assigned to be intracellular [8,10,11]. In solid-state NMR of oriented lipid bilayer samples, 3-D structural coordinates are determined directly from the NMR data relative to an external reference, namely the lipid bilayer normal, which is set parallel to the magnetic field by the method of sample preparation. As a result, the 3-D structure of the M2 peptide is fixed within the lipid bilayer, and inherently contains the helix tilt and helix rotation information. This implies that the solid-state NMR structure must be viewed as a supramolecular assembly, together with the bilayer membrane.

A molecular model of the AChR channel pore, constructed from the solid-state NMR 3-D structure of the AChR M2 helix in the membrane, and assuming a symmetric pentameric organization of the channel is shown in Fig. 4a (end view) and Fig. 4b (side view). The optimized parallel, five-helix bundle has a right handed, interhelical twist with an orientation angle of 12°. A Na^{+} is confined in the central narrow pore, which has a diameter ranging from about 3.0 Å at its narrowest, to 8.6 Å at its widest (Fig. 4a). Nonpolar residues are predominantly on the exterior of the bundle, while polar residues line the pore. This arrangement is in agreement with evidence collected from mutagenesis, affinity labeling and cysteine accessibility measurements [8,10,11,15–20]. Specifically, cysteine scanning [18] identified eight residues accessible to modification by methane thiosulfonate reagents in M2 of the AChR α subunit in the open channel: Glu-1, Thr-4, Ser-8, Leu-11, Ser-12, Val-15, Leu-18, and Glu-22. Five of these residues are exposed to the pore lumen in the structure shown in Fig. 4a: Glu-1, Ser-4, Ser-8, Val-15, Leu-18, and Gln-22. A side view (Fig. 4b) shows a funnel-shaped

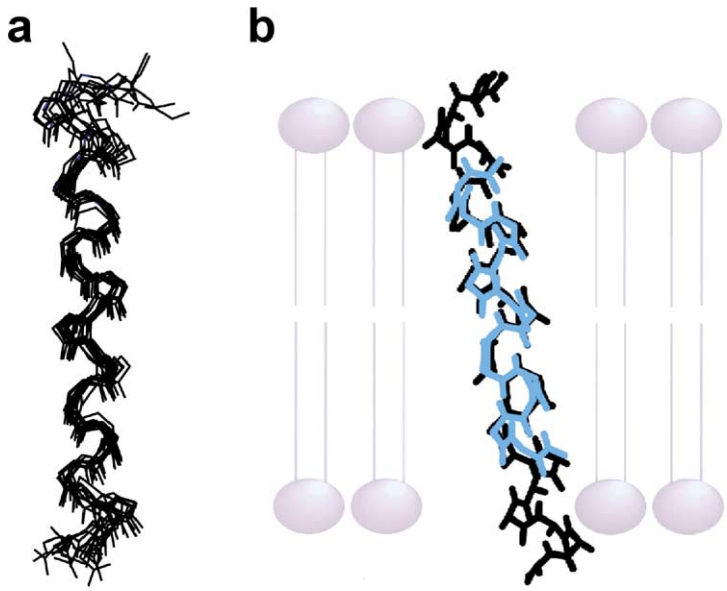

Fig. 3. (a) Superposition of the backbone heavy atoms for the 10 lowest energy structures of AChR M2 determined by solution NMR in DPC micelles. (b) Superposition of the average structure of the AChR M2 calculated from the solution NMR distance constraints (black), and the average structure determined from the solid-state NMR orientational constraints (cyan). Both structures are shown in the bilayer membrane, in the exact overall orientation determined from solid-state NMR.

bundle, 33 Å in length, with the wide mouth at the N-terminus, which is assigned to be intracellular in keeping with the wealth of biochemical and mutagenesis information [8]. The profile of the ion-conduction pore calculated from the structure shows a wide infundibulum leading to two narrow constrictions generated by rings of Val-15 and Gln-22, with hole radii of 2.9 and 1.5 Å, respectively [8]. The channel lining hydroxyl residues are in agreement with the expectations of a water-filled pore, and the constrictions are compatible with the permeation of both Na^+ and K^+ ions (ionic radii of 0.95 and 1.33 Å, respectively). Remarkably, replacement of Glu-1 by Ala, Val-15 by Thr, and insertion of a proline immediately preceding Glu-1 in homomeric neuronal α7 AChRs converts the channel ionic selectivity from cationic to anionic [15,16]. The wide cavity delimited between Ser-8 and Val-15 is consistent with the binding pocket for open channel blockers [20]. Therefore, a pentameric M2 helical bundle may represent the structural blueprint for the inner bundle that lines the pore of the AChR channel. Indeed, the 4.6 Å electron diffraction map of the closed AChR channel shows the occurrence of two rings of conserved hydrophobic residues generating a belt around the pore: one ring formed by Leu-11 and the other by Val-15, separated by one turn of helix. Unwin [21,22] suggested that this may represent the structure of a hydrophobic gate that would hinder the dehydration of ions and render them too large to pass through the central pore.

Overall, the structural features of the five-helix bundle of the AChR M2 shown in Fig. 4a and b are similar to those identified in the crystal structures of the tetrameric pore of the K channel KcsA [2] and the pentameric pore of the mechanosensitive channel *MscL* [3]. The ion-conducting pathway is formed by helical bundles packed around a central pore; the pores have a funnel-like architecture, with each subunit contributing two transmembrane α-helical segments, tilted by $\sim 25^\circ$ with respect to the bilayer normal; the helices pack together as right-handed helical bundles. The pentameric pore of *MscL* [3] bears striking resemblance to the pentameric AChR M2 bundle: the N-terminal transmembrane helix of *MscL* (TM1) forms the channel lining and exposes to the pore lumen a number of hydroxyl-containing polar residues: Thr-25, Thr-28, Thr-32, and Thr-35. Two hydrophobic residues (Ile-14 and Val-21), two turns of helix apart, create a constriction near the cytoplasmic surface at the N-terminus of TM1. Thus, the sequence and amphipathic character of the TM1 helix, orientation, packing, and tilt angle are ostensibly similar to the AChR M2 helix. The occurrence of a pore constriction formed by hydrophobic residues in the presumed closed channel is reminiscent of that in the AChR M2 bundle and it may be critical for channel opening if that were to involve a rotation of the M2 helices, thereby repositioning the occluding hydrophobic residues to a permissive location. Helix rotations and changes in tilt angle have been implicated in the mechanism of channel gating both for ligand-gated [21] and voltage-gated [33,34] channels. For KcsA, a site-directed spin labeling and EPR spectroscopy study has discerned such a motion in TM2 helix that displaces it away from the conducting pathway and results in a widening of a pore at its narrowest constriction [35].

The earlier finding that the M2 segments of the glycine receptor (GlyR) family form anion-selective channels in

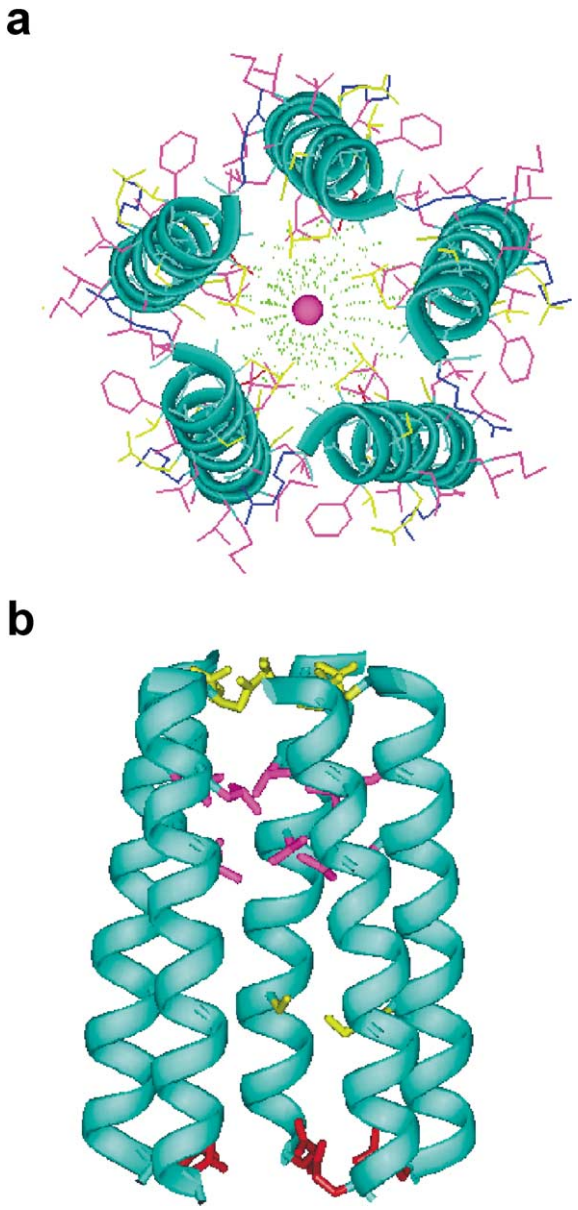

Fig. 4. Top (a) and side (b) views of a model of the AChR M2 funnel-like pentameric bundle. The channel architecture was calculated using the solid-state NMR 3-D coordinates of the M2 helix in the lipid bilayer, and by imposing a symmetric pentameric organization. The top view (a) has the C-terminal synaptic side in front. The wide mouth of the funnel is on the N-terminal, intracellular side of the pore. A sodium ion is confined within the pore. The side view (b) has the C-terminus on top; only the side chains of the pore-lining residues, Glu-1, Ser-8, Val-15, Leu-18, and Gln-22, are shown. The α-carbon backbone is shown using ribbon diagrams and depicted in cyan; acidic residues in red; basic residues in blue; polar residues in yellow; and lipophilic residues in purple. Other details are as described in Ref. [8].

lipid bilayers [36], and are transmembrane α-helices as determined by NMR spectroscopy [37,38], supports the structural kinship of AChR and GlyR. Remarkably, the inverse three mutations that convert the homomeric neuronal α7 AChRs from cation-selective to anion-selective (Ala-1 by Glu, Thr-15 by Val, and insertion of a proline immediately preceding Ala-1) [15], when introduced into M2 of the Cl^- conducting homomeric α1 GlyR converted it from anion-selective to cation-selective [39]. It is therefore plausible that a pentameric M2 helical bundle represents the blueprint for the structure that lines the pore of Gly-gated Cl^- channels.

What the structure of the M2 bundle is in the context of the intact AChR subunit within the pentameric complex remains to be established. In the meantime, this issue may be assessed through the effects of mutations identified in human diseases which alter the functional properties of the mutant receptor. A case in point is nocturnal frontal lobe epilepsy: Ser-8, a key residue exposed to the pore lumen is mutated to Phe in the neuronal α4 AChR subunit; in oocyte expression experiments, the mutated human α4 AChR exhibits increased affinity for ACh and increased rate of desensitization [40,41]. For M2 of the GlyR α1, a mutation of Gln-15 (a position equivalent to that of the critical Val-15 in the AChR M2) for His is associated with hyperekplexia (Startle disease) [42,43]. This is precisely what the pentameric M2 helical bundle model would predict.

4. Concluding remarks

We have described a hierarchical strategy to elucidate sequence-structure determinants by investigating autonomously folded modules in the absence of the entire channel protein. This endeavor has led to the determination of the structure of the channel lining segments of neurotransmitter-gated channels in membranes. The advances reviewed set us on a solid framework to proceed to the determination of the structure of an intact channel protein embedded in membranes by NMR spectroscopy.

Acknowledgements

This review summarizes work done in collaboration with F. Marassi, J. Gesell, A. Valente, Y. Kim, and M. Oblatt-Montal. The original findings appeared in Ref. [8]. This research was supported by grants from the National Institute of General Medical Sciences to M.M. and S.J.O. (GM-49711, GM-56538) and utilizes the Resource for Solid-State NMR of Proteins at the University of California San Diego, which is supported by National Institutes of Health grant P41RR09793.

References

[1] T.D. Albright, T.M. Jessell, E.R. Kandel, M.I. Posner, Neuron 25 (2000) S1–S55 (Supplement).
[2] D.A. Doyle, J. Morais Cabral, R.A. Pfuetzner, A. Kuo, J.M. Gulbis, S.L. Cohen, B.T. Chait, R. MacKinnon, Science 280 (1998) 69–77.
[3] G. Chang, R.H. Spencer, A.T. Lee, M.T. Barclay, D.C. Rees, Science 282 (1998) 2220–2226.

[4] D. Fu, A. Libson, L.J. Miercke, C. Weitzman, P. Nollert, J. Krucinski, R.M. Stroud, Science 290 (2000) 481–486.
[5] H. Sui, B.G. Han, J.K. Lee, P. Walian, B.K. Jap, Nature 414 (2001) 872–878.
[6] R. Dutzler, E.B. Campbell, M. Cadene, B.T. Chait, R. MacKinnon, Nature 415 (2002) 287–294.
[7] F.C. Almeida, S.J. Opella, J. Mol. Biol. 270 (1997) 481–495.
[8] S.J. Opella, F.M. Marassi, J.J. Gesell, A.P. Valente, Y. Kim, M. Oblatt-Montal, M. Montal, Nat. Struct. Biol. 6 (1999) 374–379.
[9] B. Hille, Ion Channels of Excitable Cells, 3rd ed., Sinauer, Sunderland, MA, 2001.
[10] P.J. Corringer, N. Le Novere, J.P. Changeux, Annu. Rev. Pharmacol. Toxicol. 40 (2000) 431–458.
[11] V. Itier, D. Bertrand, FEBS Lett. 504 (2001) 118–125.
[12] K. Brejc, W.J. van Dijk, R.V. Klaassen, M. Schuurmans, J. van Der Oost, A.B. Smit, T.K. Sixma, Nature 411 (2001) 269–276.
[13] A. Miyazawa, Y. Fujiyoshi, M. Stowell, N. Unwin, J. Mol. Biol. 288 (1999) 765–786.
[14] P.N. Kao, A.J. Dwork, R.R. Kaldany, M.L. Silver, J. Wideman, S. Stein, A. Karlin, J. Biol. Chem. 259 (1984) 11662–11665.
[15] J.L. Galzi, A. Devillers-Thiery, N. Hussy, S. Bertrand, J.P. Changeux, D. Bertrand, Nature 359 (1992) 500–505.
[16] P.J. Corringer, S. Bertrand, J.L. Galzi, A. Devillers-Thiery, J.P. Changeux, D. Bertrand, Neuron 22 (1999) 831–843.
[17] M.H. Akabas, C. Kaufmann, P. Archdeacon, A. Karlin, Neuron 13 (1994) 919–927.
[18] G. Wilson, A. Karlin, Proc. Natl. Acad. Sci. U. S. A. 98 (2001) 1241–1248.
[19] C. Labarca, M.W. Nowak, H. Zhang, L. Tang, P. Deshpande, H.A. Lester, Nature 376 (1995) 514–516.
[20] P. Charnet, C. Labarca, R.J. Leonard, N.J. Vogelaar, L. Czyzyk, A. Gouin, N. Davidson, H.A. Lester, Neuron 4 (1990) 87–95.
[21] N. Unwin, Philos. Trans. R. Soc. Lond., B. Biol. Sci. 355 (2000) 1813–1829.
[22] N. Unwin, Nature 373 (1995) 37–43.
[23] J. Corbin, N. Methot, H.H. Wang, J.E. Baenziger, M.P. Blanton, J. Biol. Chem. 273 (1998) 771–777.
[24] N. Methot, B.D. Ritchie, M.P. Blanton, J.E. Baenziger, J. Biol. Chem. 276 (2001) 23726–23732.
[25] S. Oiki, W. Danho, V. Madison, M. Montal, Proc. Natl. Acad. Sci. U. S. A. 85 (1988) 8703–8707.
[26] S. Oiki, V. Madison, M. Montal, Proteins 8 (1990) 226–236.
[27] R.J. Law, L.R. Forrest, K.M. Ranatunga, P. La Rocca, D.P. Tieleman, M.S. Sansom, Proteins 39 (2000) 47–55.
[28] M. Oblatt-Montal, L.K. Buhler, T. Iwamoto, J.M. Tomich, M. Montal, J. Biol. Chem. 268 (1993) 14601–14607.
[29] M.O. Montal, T. Iwamoto, J.M. Tomich, M. Montal, FEBS Lett. 320 (1993) 261–266.
[30] F.M. Marassi, J.J. Gesell, A.P. Valente, Y. Kim, M. Oblatt-Montal, M. Montal, S.J. Opella, J. Biomol. NMR 14 (1999) 141–148.
[31] T.A. Cross, Methods Enzymol. 289 (1997) 672–696.
[32] S.J. Opella, C. Ma, F.M. Marassi, Methods Enzymol. 339 (2001) 285–313.
[33] A. Grove, M.S. Montal, G.L. Reddy, S. Marrer, T. Iwamoto, J. Tomich, M. Montal, in: A.B. Pullman, B. Pullman, J. Jortner (Eds.), Twenty Fifth Jerusalem Symposium. Membrane Proteins: Structures, Interactions and Models, Kluwer Academic Publishing, Amsterdam, The Netherlands, 1992, pp. 249–268.
[34] F. Bezanilla, Physiol. Rev. 80 (2000) 555–592.
[35] Y.S. Liu, P. Sompornpisut, E. Perozo, Nat. Struct. Biol. 8 (2001) 883–887.
[36] G.L. Reddy, T. Iwamoto, J.M. Tomich, M. Montal, J. Biol. Chem. 268 (1993) 14608–14615.
[37] S.J. Opella, J. Gesell, A.P. Valente, F.M. Marassi, M. Oblatt-Montiel, A.V. Ferrer-Montiel, W. Sun, M. Montal, Chemtracts 10 (1997) 153–174.
[38] M. Montal, S.J. Opella, Assembly Properties of Model Transmembrane Channel Peptides, R.G. Landes, Austin, TX, 1997.
[39] A. Keramidas, A.J. Moorhouse, C.R. French, P.R. Schofield, P.H. Barry, Biophys. J. 79 (2000) 247–259.
[40] S. Weiland, V. Witzemann, A. Villarroel, P. Propping, O. Steinlein, FEBS Lett. 398 (1996) 91–96.
[41] S. Weiland, D. Bertrand, S. Leonard, Behav. Brain Res. 113 (2000) 43–56.
[42] J.W. Lynch, S. Rajendra, K.D. Pierce, C.A. Handford, P.H. Barry, P.R. Schofield, EMBO J. 16 (1997) 110–120.
[43] R.S. Shiang, Y.Z. Zhu, A.F. Hahn, P. O'Connell, J.J. Wasmuth, Nat. Genet. 5 (1993) 351–358.